

Research Article

Microfabrication and Magnetic Particle Spectrometry of Magnetic Discs

Per A. L othman^a · Thomas Janson^a · Yannick Klein^a · Andr e-Ren e Blaudszun^a · Michael Ledwig^b · Leon Abelmann^{a,*}

^aKIST Europe, Saarbr ucken, Germany

^bPure Devices, W urzburg, Germany

*Corresponding author, email: l.abelmann@kist-europe.de

Received 25 November 2016; Accepted 20 June 2017; Published online 11 July 2017

  2017 Abelmann; licensee Infinite Science Publishing GmbH

This is an Open Access article distributed under the terms of the Creative Commons Attribution License (<http://creativecommons.org/licenses/by/4.0>), which permits unrestricted use, distribution, and reproduction in any medium, provided the original work is properly cited.

Abstract

We report on the fabrication of dispersions of Au/Ni₈₁Fe₁₉/Au magnetic discs with two and three micrometer diameter and thickness in the order of hundred nanometers. The magnetisation reversal of the discs was analysed on a time-scale of an hour as well as a few milliseconds to assess their suitability for magnetic particle imaging. We conclude that compared to FeraSpin particles, these microfabricated particles saturate in fields as low as 12 mT, the shape of the hysteresis loop is relatively independent of the field sweep rate, and the difference in phase between higher harmonics is constant up to the 20th harmonic. These radically different magnetic properties suggest that microfabricated particles might have advantages for applications such as magnetic particle imaging.

1. Introduction

All tracer particles used today for magnetic particle imaging (MPI) are synthesised by colloidal chemistry [1]. This situation is analogous to the early days of magnetic data storage, when all magnetic recording layers were based on pigments [2]. The advent of thin film deposition techniques revolutionised the field. Moving away from magnetic oxides, first to metal alloys and later to intricate multilayered structures, led to a ten million fold increase in data density. The field of magnetic particle imaging could benefit significantly from the developments in the magnetic thin film community. To obtain particle suspensions, the films have to be patterned. One might object that the patterning technique will render the fabrication of particles prohibitory expensive. In magnetic hard disc recording, however, research into bit patterned media has led to cost effective patterning down to the nanometer scale [3]. Assuming that the hard disc drive industry could produce 100 mm diameter bit patterned

discs for a few euros, then the cost of production would be in the order of 10 Euro per milligram magnetic material. Therefore, microfabricated particles for biomedical applications are an economically a viable option.

The first attempts to create dispersions of micrometer sized particles have been reported [4, 5], addressing hyperthermia treatment and mechano-stimulation. Application as tracer particles in magnetic particle imaging has not been investigated yet. It should be noted that particles of micrometer size are most likely not suitable for clinical use. When inserted in the bloodstream, this size of particle will end up in the lungs. Microfabrication however allows for particles with dimensions in the order of 50 nm, similar to approved solutions like Resovist. However, we believe it does make sense to start investigating micrometer sized particles since they are much easier to observe and handle. Using these bigger particles we can tackle the first problems in fabrication, and assess the potential of microfabricated particles in MPI.

In this contribution, we introduce particles made by

lithography-based micro-fabrication for MPI. Microfabricated particles offer freedom in the design of their shape as well as the choice of their magnetic layer composition, thickness and stacking with non-magnetic layers. This opens ways to tailor the shape of the hysteresis loop, and optimise the harmonic response for MPI. We describe the fabrication process of simple permalloy ($\text{Ni}_{81}\text{Fe}_{19}$) disc of 2 and 3 μm diameter (see Fig. 1), covered with gold on both sides for protection and optional surface functionalization, on which we show the first results of magnetic particle spectroscopy.

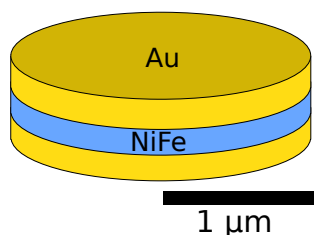


Figure 1: Schematic view of a microfabricated magnetic disc with gold outer surfaces. The thickness of the gold layers is kept approximately equal to that of the NiFe alloy layer, varying from 7 to 54 nm.

II. Experimental

Fabrication

The initial steps of the fabrication of microfabricated particles are relatively straightforward, see Fig. 2. A pre-diced crystalline silicon wafer is used as carrier (Step 1), onto which a negative photoresist (Olin908-Ti 35 ES) is spin-coated to a thickness of 3.0(5) μm (Step 2).

On top of this polymer sacrificial layer, the metal stack is deposited (Step 3), consisting of the magnetic $\text{Ni}_{81}\text{Fe}_{19}$ thin film, sandwiched between two Au films of equal thickness. The films are deposited in a load-locked vacuum system (VSW technology) by means of 2 inch magnetron sputter guns at a distance of 10 cm from the substrate. The base pressure in the system was 0.6(2) μPa , the Ar pressure during sputtering of 1.00(1) Pa is controlled by a butterfly throttle valve. The Au and $\text{Ni}_{81}\text{Fe}_{19}$ films were sputtered using a DC supply at 30 W power, resulting in a deposition rate of 214(2) pm/s and 69(9) pm/s respectively (measured in the centre of the wafer). During deposition the substrate is rotated at 15 rpm to promote thickness uniformity and avoid any magnetically induced anisotropy. The substrates are in contact with a substrate holder at room temperature.

After a dehydration bake of 5 min at 120 $^{\circ}\text{C}$ the metal stack is treated with a priming liquid (HMDS), covered with a positive photoresist (Olin oir 907-17), which is baked out for 90 s at 90 $^{\circ}\text{C}$, exposed through a contact mask, and baked out again for a total of 11 min at 120 $^{\circ}\text{C}$

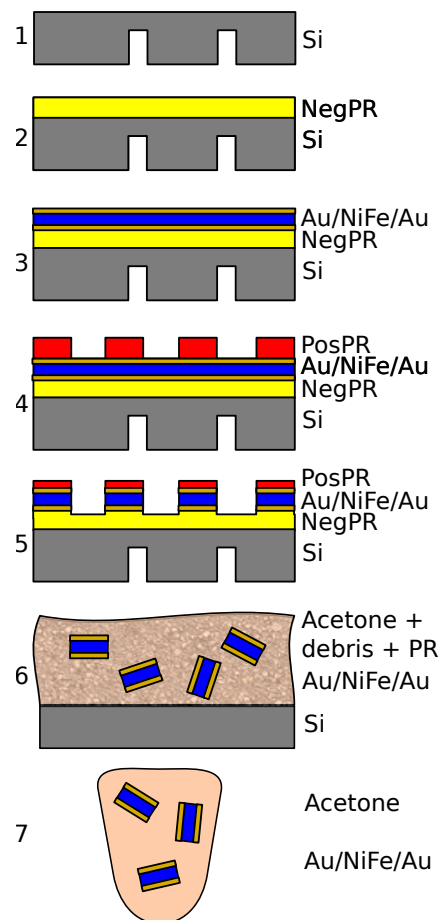


Figure 2: Schematic process view. The discs are fabricated on a pre-diced silicon wafer (1). The Au/NiFe/Au stack is sputter deposited (3) on a sacrificial layer (2), which is patterned by contact lithography (4, 5) into discs of 2 μm diameter. Because of the polymer sacrificial layer, these discs can be easily released from the wafer and dispersed in acetone (6). For this the wafer is broken in smaller parts using the grooves on the back. The particles are transferred to a tube and washed several times (7) before use.

(Step 4). The metal stack has therefore experienced a thermal load of approximately 16 min at 120 $^{\circ}\text{C}$.

The positive photoresists is developed in OPD4262. Since the negative photoresist is exposed, if not during transport and storage, then certainly by the plasma in the sputtering system, it is resistant against the positive photoresist developer. The resulting photoresist pattern of a rectangular array of 2 or 3 μm diameter discs spaced centre-to-centre at twice the diameter is transferred into the metal stack using ion beam etching (IBE, Oxford i300) using ion detection (SIMS) end-point detection (Step 5).

The wafer is broken using the pre-diced grooves on the backside, and dies of about a quarter wafer are flooded with acetone, while preventing the acetone from spilling over the edges of the die. The negative photoresist layers dissolve, releasing 68×10^6 2 μm or 30×10^6

3 μm diameter multilayered discs per wafer die (Step 6). These discs are sucked by a pipette from the wafer and collected in a 0.2 mL polypropylene reaction tube. The particles are ultrasonically agitated for 30 min and rinsed five times with acetone using magnetic concentration to separate the discs from the liquid (Step 7).

Microscopic characterisation

Fig. 3 shows a cross section of the metal layer stack. For clarity, the layers in the images are thicker than those finally used in the disc. The cross section was made after focussed ion beam (FIB) etching a hole into the wafer (FEI Nova 600). To protect the metal layers (for making the cross-section only), a Pt cover was deposited by chemical vapour deposition (CVD) inside the FIB/SEM, before etching the hole. This Pt projection layer consists of two layers. First, a 0.8 μm Pt layer was deposited by electron beam induced CVD, after which a 3 μm layer was deposited by ion beam induced CVD. In this way, there is minimal damage to the metal layers. The image is corrected by image treatment for the 52° observation tilt of the scanning electron microscopy (SEM). The interfaces between the individual layers are well defined and appear smooth.

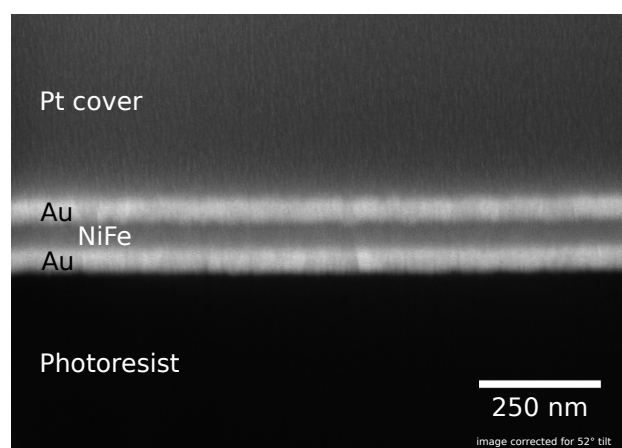


Figure 3: SEM cross section view of a Au(50 nm)/NiFe(54 nm)/Au(50 nm) layer stack, still on the sacrificial photoresist layer on the fabrication wafer. The cross section was produced by focussed ion beam milling. The stack is protected with a thick Pt layer against damage from the ion beam. This Pt layer is not present on the fabricated discs.

An optical micrograph of an array of 3 μm diameter fabricated discs, still on the handling wafer, is shown in Fig. 4. To reveal the surface of the discs, the top photoresist layer was removed by a cotton stick drenched in acetone. In the centre of the discs, small holes can be observed. These holes were occasionally also observed by scanning electron microscopy (SEM), transmission electron microscopy (TEM) and atomic force microscopy (AFM). We believe these holes are most likely caused by a

height difference in the photoresist (thicker at the edge), and a slight over-etching in the IBE.

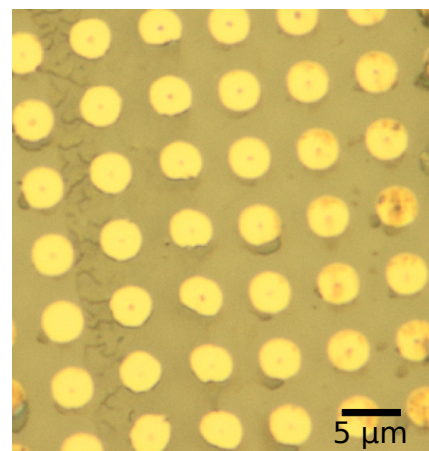


Figure 4: Optical microscopy image of a part of the array of microfabricated discs still on the fabrication wafer.

Fig. 5 shows an optical microscopy image of 3 μm diameter Au(5 nm)/NiFe(7.2(4) nm)/Au(5 nm) particles that were transferred from acetone into a water droplet. A rotating, external magnetic field was applied by a small permanent magnet mounted on a motor. In the additional material, a video of the response of the particles to the field is shown. Under application of the external field, the particles align with their rims touching, and form bigger clusters. This alignment might influence the magnetic response, and requires further investigation.

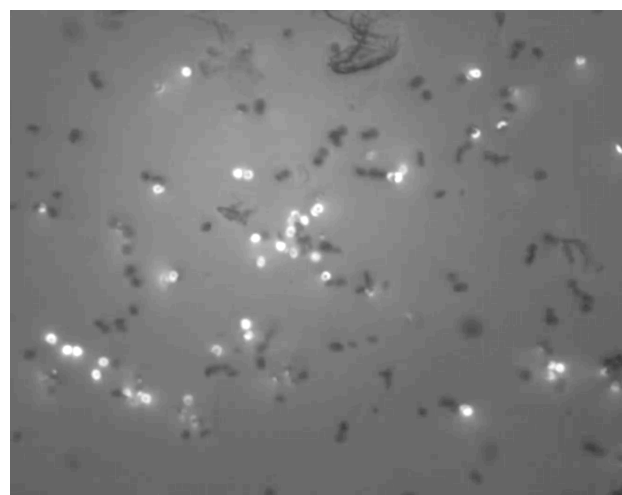


Figure 5: Optical microscope image of 3 μm diameter Au(5 nm)/NiFe(7 nm)/Au(5 nm) discs inside a water droplet. See additional material for video images of the reaction of these particles to an external magnetic field.

Fig. 6 shows a top view scanning electron microscopy image of a 2 μm Au(5 nm)/NiFe(7 nm)/ Au(5 nm) disc after drying a droplet of the suspension in buffered phos-

phate saline (PBS) on a silicon wafer. In this particular case, the holes that were observed in Fig. 4 are not apparent.

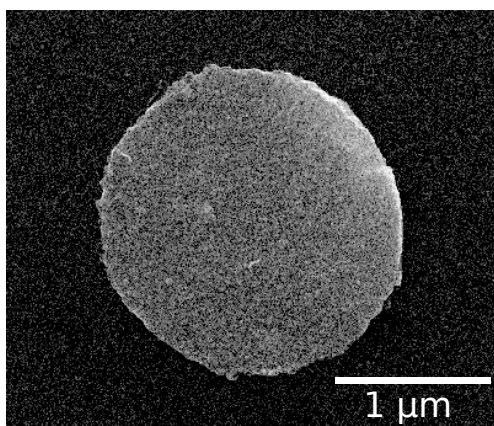


Figure 6: Scanning Electron Microscopy image of a 2 μm diameter Au(5 nm)/NiFe(7 nm)/Au(5 nm) disc.

Magnetic characterisation

The quasi-static magnetic hysteresis loops were measured on continuous or patterned films on 7 mm \times 7 mm dies from the silicon carrier wafer in a vibrating sample magnetometer (MicroSense VSM-10). The dynamic magnetic response of the microfabricated particles dispersed in ethanol was determined in a Pure Devices magnetic particle spectrometer (MPS). The NiFe layer thicknesses was increased from 7 to 12 nm to increase the magnetic signal. To ensure particle integrity, also the gold thicknesses were increased. There was, within measurement error, no difference between discs of 2 or 3 μm diameter.

From the 0.2 mL solution of 68×10^6 particles, 0.03 mL was inserted into a 4 mm tube to obtain the magnetic response, which corresponds to approximately 10×10^6 particles. The drive frequency was 20 140 Hz and the spectral response was recorded up to the 50th harmonic. A total of 50 individual measurements were averaged. Between the measurements, the sample was taken out of the device (automatically), to correct for drift by subtracting the background signal. Again, no clear difference between 2 and 3 μm particles could be observed. For comparison a 100 mmol/L solution of FeraSpin R was measured.

III. Results and Discussion

After lithography, the magnetic particles are still arranged in a square array on the support wafer (Step 5 in Fig. 2). By pre-dicing the wafer, we produced dies on which the total number of particles is known *exactly*. These dies are used for vibrating sample magnetometry (VSM). Fig. 7

shows the quasi-static VSM hysteresis loop, measured over a total period of 140 min, as well as the dynamic loop deduced from magnetic particle spectrometry, measured within 5 ms. For comparison of their shapes, both loops have been normalised to their maximum signal. In contrast to super-paramagnetic particles, which show orders of magnitude increase in coercivity with increasing field sweep rate, both the slow and fast hysteresis loops are nearly identical. The coercivity only increases by 60 % (from 1.7(1) mT to 2.7(6) mT), and the small shoulder visible in the VSM loop near saturation disappeared. This is a surprising result, considering that there is a seven order of magnitude difference in field sweep rate, and the fact that the particles are either fixed and perfectly aligned (VSM), or dispersed randomly in a liquid (MPS). The remanence of the microfabricated particles is high, with a squareness ratio (M_r/M_s) of 0.59(5). Since the particles are also remanent in static magnetic fields, they will attract each other and agglomeration might be a problem. In acetone, the particles are easily dispersed by shaking the tube. In a microfluidic chip however (see Fig. 5), the particles remain connected after removing the field. This effect might be an issue in MPI, since agglomeration will change the magnetic response.

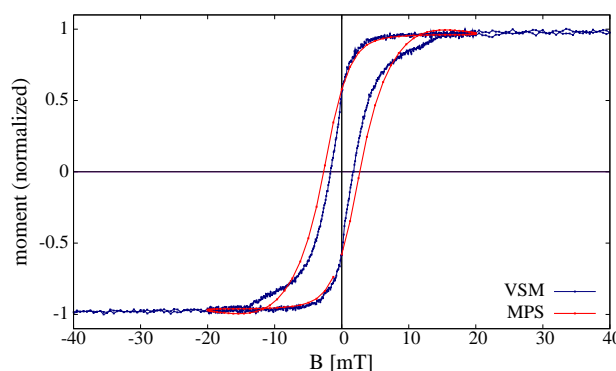


Figure 7: Hysteresis loop of an array of microfabricated Au(14 nm)/NiFe(12 nm)/Au(14 nm) discs on the carrier wafer measured quasi-statically in a vibrating sample magnetometer (loop duration 140 min) and at 20 kHz in a magnetic particle spectrometer. There is no essential difference in loop shape.

Both the VSM and MPS give accurate values of the total magnetic moment, respectively 137(3) nAm² for 4×10^6 particles and 380(10) nAm² for 10×10^6 particles. The magnetic moment per particle is slightly lower for the VSM measurement ($3.43(7) \times 10^{-14}$ Am²) than for the MPS ($3.8(1) \times 10^{-14}$ Am²). From the Ni₈₁Fe₁₉ thickness of 12(2) nm, particle diameter of 2 μm and assuming a bulk value saturation magnetisation of 820 kA/m, we can estimate a theoretical moment per particle of $3.0(5) \times 10^{-14}$ Am². It therefore appears as if the MPS is overestimating the particle moment. The most likely explanation is inaccuracy in pipetting the 30 μL from the

Eppendorf tube into the glass tube of the MPS. In any case, we can conclude that there are not many particles lost when transferring the particles from the carrier wafer into the tube.

Fig. 8 shows the normalised MPS spectrum of the microfabricated particles again, but now compared to a standard solution (FeraSpin R). The FeraSpin R hysteresis loop is far from being saturated at 20 mT. In contrast, the microfabricated particles already saturate at approximately 12 mT. It is expected this rapid saturation can be used to increase the resolution in MPI. The coercivities of both suspensions are nearly identical, but it should be noted that the coercivity of the FeraSpin is highly dependent on the applied field value.

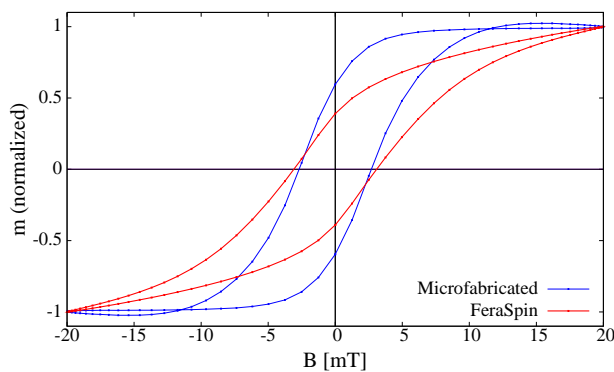


Figure 8: Hysteresis loop of a dispersion of approximately 10^7 microfabricated particles dissolved in acetone, measured by magnetic particle spectroscopy at 20 kHz, compared to a FeraSpin R reference sample. For ease of comparison of the loop shapes, both curves were normalised. Compared to the FeraSpin particles, the hysteresis loop of the microfabricated particles has higher squareness and already saturates at about 12 mT.

Fig. 9 shows the magnetic spectra measured at a field sweep amplitude of 20 mT on both the microfabricated and FeraSpin particle dispersions. The signal was normalized to the amount of magnetic atoms (Fe in the case of FeraSpin, and Ni plus Fe in the case of the microfabricated particles). For the normalization of FeraSpin, we assumed the concentration of 100 mmolL^{-1} to be correct and an amount of $30 \mu\text{L}$ in the MPS. For an estimate of the amount of magnetic material in the MMP suspension, we start from the VSM value of the moment per disc ($3.43(7) \times 10^{-14} \text{ Am}^2$). From the MPS signal of 375 nAm^2 we conclude there were 11×10^6 discs in the system. Assuming a disc diameter of $2 \mu\text{m}$ and a film thickness of 12 nm of $\text{Ni}_{81}\text{Fe}_{19}$ with density $8.71 \times 10^3 \text{ kg/m}^3$ and 58.1 g/mol obtained from simple mixing, we estimate a total of 61.7 nmol of nickel and iron atoms in the system. Under these assumptions, the magnetic moment of the microfabricated particles per mol of magnetic atom is about 20% higher than that of FeraSpin ($6(1) \text{ Am}^2/\text{mol}$

versus $5(1) \text{ Am}^2/\text{mol}$).

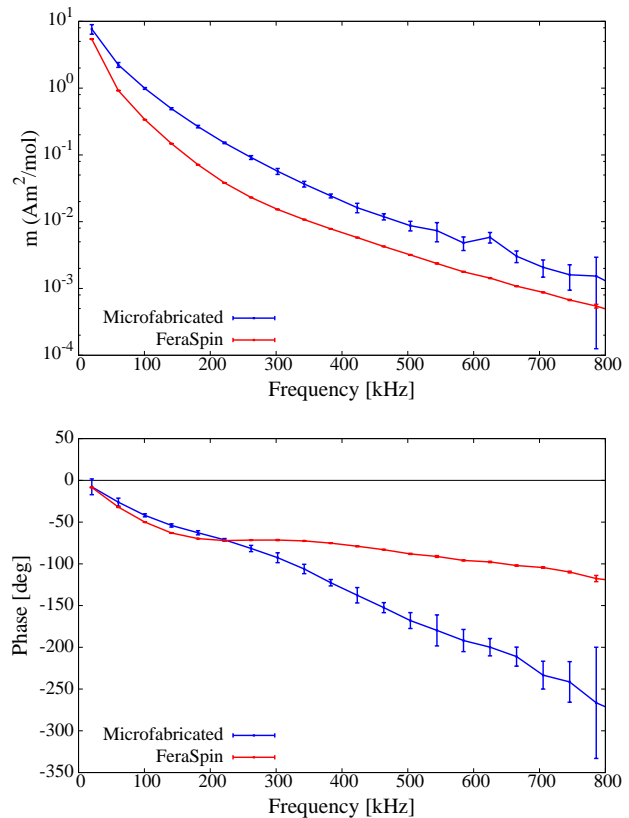


Figure 9: Spectra measured by magnetic particle spectroscopy at 20 kHz. The decay in harmonic amplitude with number is similar for the microfabricated particles and FeraSpin R. In comparison to the FeraSpin R reference sample, however, the relation between phase and harmonic number is more linear for the microfabricated discs.

The decay of the amplitude of the harmonics with harmonic number is equal for both dispersions. However, the phase relations between the harmonics are very different. For the FeraSpin dispersion, the phase flattens off at approximately 80° after the 4th harmonic. The phase of the harmonics of the microfabricated continuously increases with $15(2)^\circ$ per harmonic all the way up to the 20th harmonic, after which the signal reaches the noise floor. This particular behaviour could perhaps be exploited to increase MPI sensitivity.

IV. Conclusions

We have prepared magnetic discs of 2 and $3 \mu\text{m}$ diameter from a Au/NiFe/Au multilayered film by lithography and ion beam etching on a sacrificial polymer film. By lift-off, these discs were dispersed into acetone.

The time dependency of the hysteresis loop of a solution of microfabricated particles is very different from that of commonly used colloidal particles. In contrast to

those super-paramagnetic particles, the shape of the hysteresis loop measured by magnetic particle spectrometry at 20 kHz is very similar to the quasi-static loop measured by vibrating sample magnetometry, with a coercivity of the MPS loop that is only 60% higher.

Compared to magnetic particle spectrometry measurement of a standard FeraSpin R solution, the microfabricated particles have identical coercivity, but are already completely saturated at 12 mT. The decay in amplitude of the higher harmonics is identical for the FeraSpin R and the microfabricated particles. The phase relation between the harmonic is however significantly more constant for the microfabricated particles, with an increase of $15(2)^\circ$ per harmonic.

The domain wall based reversal behaviour of these microfabricated magnetic particles leads to a particular magnetic response that may have advantages for magnetic particle imaging, possibly leading to higher contrast and resolution.

Acknowledgements

The authors would like to thank Ke-Chun Ma of Micro-Create, The Netherlands, for cleanroom fabrication and

metrology, Henk van Wolferen of Twente University, for FIB/SEM cross-section analysis, Thijs Bolhuis of Twente University for VSM, Carsten Brill of KIST Europe for SEM imaging, Tijmen Hageman of KIST Europe for optical microscopy and Andreas Manz and Marc Pichel of KIST Europe for valuable discussions.

References

- [1] R. M. Ferguson, A. P. Khandhar, and K. M. Krishnan. Tracer design for magnetic particle imaging (invited). *J. Appl. Phys.*, 111(7):07B318, 2012. doi:[10.1063/1.3676053](https://doi.org/10.1063/1.3676053).
- [2] E. D. Daniel, C. D. Mee, and M. H. Clark. *Magnetic Recording: The First 100 Years*. Wiley-IEEE Press, Hoboken, 1998.
- [3] J. Lille, K. Patel, R. Ruiz, T.-W. Wu, H. Gao, L. Wan, G. Zeltzer, E. Dobisz, and T. R. Albrecht. Imprint lithography template technology for bit patterned media (BPM). In *SPIE Photomask Technology*, 2011. doi:[10.1117/12.898785](https://doi.org/10.1117/12.898785).
- [4] E. A. Rozhkova, V. Novosad, D.-H. Kim, J. Pearson, R. Divan, T. Rajh, and S. D. Bader. Ferromagnetic microdisks as carriers for biomedical applications. *J. Appl. Phys.*, 105(7):07B306, 2009. doi:[10.1063/1.3061685](https://doi.org/10.1063/1.3061685).
- [5] S. Leulmi, H. Joisten, T. Dietsch, C. Iss, M. Morcrette, S. Auffret, P. Sabon, and B. Dieny. Comparison of dispersion and actuation properties of vortex and synthetic antiferromagnetic particles for biotechnological applications. *Appl. Phys. Lett.*, 103(13):132412, 2013. doi:[10.1063/1.4821854](https://doi.org/10.1063/1.4821854).